agronomy

Article

Optimization of N Fertilizer Type and Ridge–Furrow Ratio to Improve Resource Use Efficiency and Grain Yield of Rain-Fed Winter Wheat in Loess Plateau, China

Shengcai Qiang [1,2], Yan Zhang [1,2], Junliang Fan [3,*], Fucang Zhang [3], Wen Lin [2], Min Sun [2], Zhiqiang Gao [2] and Xiwang Tang [4]

[1] College of Urban and Rural Construction, Shanxi Agricultural University, Taigu 030801, China; qiangsc7631231@163.com (S.Q.); zhangyan2729@163.com (Y.Z.)
[2] Ministerial and Provincial Co-Innovation Centre for Endemic Crops Production with High-Quality and Efficiency in Loess Plateau, Shanxi Agricultural University, Taigu 030801, China; slwrdewy@163.com (W.L.); sm_sunmin@126.com (M.S.); gaozhiqiang1964@126.com (Z.G.)
[3] Key Laboratory of Agricultural Soil and Water Engineering in Arid and Semiarid Areas of Ministry of Education, Northwest A&F University, Yangling 712100, China; zhangfc@nwsuaf.edu.cn
[4] Hebei Key Laboratory of Agroecological Safety, Hebei University of Environmental Engineering, Qinghuangdao 066000, China; tangxiwang@hebuee.edu.cn
* Correspondence: nwwfjl@163.com

Abstract: Ridge and furrow plastic mulch (RFPM) and nitrogen (N) application are effective strategies for improving crop productivity in China's Loess Plain. However, it is not clear how the ridge–furrow ratio and nitrogen fertilizer type (NT) affect the use of water, nitrogen, heat, and radiation resources for the enhancement of rain-fed wheat production. Two nitrogen fertilizer types (traditional urea (TU) and controlled-release urea (CRU)) and four planting patterns (conventional flat planting (F) and the RFPM system of 20 cm ridges with 40 cm furrows (R_2F_4), 40 cm ridges with 40 cm furrows (R_4F_4), and 60 cm ridges with 40 cm furrows (R_6F_4)) were tested from September 2018 to June 2021 during the winter wheat growing season. It was found that the RFPM system can increase soil thermal time (TT_{soil}) from 41.0 to 152.1 °C d compared to the F. RFPM system thermal effect, which reduced the vegetative growth period and prolonged the reproductive growth period for 2 to 7 days, which promoted an increase in the leaf area index (LAI) and final dry matter (DM) accumulation. These significantly increased the grain yield (GY) in the RFPM system by 51.6–115.2% and enhanced the thermal time use efficiency (TUE) by 48–99.5%, water productivity (WP) by 37.4–76.3%, radiation use efficiency (RUE) by 16.3–34.4%, and partial factor productivity of nitrogen (PFP_N) by 51.6–115.2% compared to F. Although a high ridge and furrow ratio in combination with CRU increased the GY and resource use efficiency, it also exacerbated the soil water depletion, especially in the soil layer between 40 and 140 cm. Overall, CRU combined with the 40 cm ridge and 40 cm furrow RFPM system maximized resource efficiency and increased wheat production on China's Loess Plateau.

Keywords: ridge–furrow ratio; nitrogen fertilizer type; winter wheat; soil hydrothermal; resource use efficiency; grain yield

Citation: Qiang, S.; Zhang, Y.; Fan, J.; Zhang, F.; Lin, W.; Sun, M.; Gao, Z.; Tang, X. Optimization of N Fertilizer Type and Ridge–Furrow Ratio to Improve Resource Use Efficiency and Grain Yield of Rain-Fed Winter Wheat in Loess Plateau, China. *Agronomy* **2024**, *14*, 172. https://doi.org/10.3390/agronomy14010172

Academic Editor: Domenico Ronga

Received: 6 December 2023
Revised: 29 December 2023
Accepted: 10 January 2024
Published: 12 January 2024

1. Introduction

The genotype of seeds is the internal factor that determines the yield potential of crops, while the water, fertilizer, temperature, solar radiation, and other exterior factors limit the yield potential [1,2]. Winter wheat (*Triticum aestivum* L.), a common pasta crop in northern China, is widely grown on the Loess Plateau [3]. The high solar radiation in this region can lead to high crop production. However, yields are often low and unstable due to the region's scarce rainfall and infertile soils [4]. Therefore, improving soil moisture and nutrient availability to match solar radiation resources is crucial for achieving greater and more stable grain yields.

The efficient storage of precipitation is an effective way to deal with the low availability of soil moisture [5]. Ridge–furrow plastic mulching (RFPM) is considered the most effective planting technology in rain-fed agricultural areas due to its ability to collect and store precipitation [4,6]. Previous studies have shown that the RFPM system facilitated precipitation infiltration, suppressed soil evaporation, increased daily radiation, and raised the soil temperature in the early stage of crop growth [7,8]. These changes improved the photosynthetic assimilation efficiency of the leaves, thus promoting the accumulation of dry matter and the yield [9,10]. The ridge–furrow ratio in the RFPM system is a critical indicator that influences resource allocation and can have a significant impact on resource utilization efficiency and final yield formation in rain-fed farming areas [6,7,11]. Increasing the ridge width can significantly improve soil water and thermal conditions. Conversely, reducing the furrow area artificially increases plant density and competition between plants, resulting in the poor use of solar radiation and heat resources and ultimately reducing the crop yield [6,12,13]. Thus, it is worth investigating the regulatory effect of the ridge–furrow ratio on crop resource utilization and yield.

The most common and effective way to improve the low soil fertility of the Loess Plateau is to apply fertilizer (especially nitrogen) [14,15]. Numerous studies have shown that N fertilizer application promotes canopy expansion [9,14], leading to the enhanced interception of radiation and its conversion into biomass, ultimately resulting in increased grain yield [16,17]. The nitrogen fertilizer type also affects crop growth, development, and crop production. The new slow-release urea (CRU) fertilizer can effectively improve soil N availability compared to traditional urea (TU) [6,15,18]. This change resulted in the extension of the root system downwards, which improved the uptake and utilization of deep soil nitrogen by the plant root system, thus reducing the mismatch between nitrogen supply and demand in the middle and late stages of the plant and ultimately delaying early leaf senescence [14]. Therefore, a higher GY can be obtained by applying CRU compared to TU [6,15,18,19]. However, there have been few studies on the vital production resources of different nitrogen fertilizer types, particularly when applying different nitrogen fertilizer types to RFPM systems.

There have been many studies on the RFPM system, the application of nitrogen to crops, and critical resource (water, nitrogen, thermal, and radiation) use efficiency [2,8,14]. However, more information is required on the combined effects of the ridge–furrow ratio and type of N fertilization (NT) on the GY and resource use efficiency of rain-fed winter wheat in China's Loess Plateau. In theory, the effects of soil moisture and nitrogen on growing and developing crops interact with each other [4,20], but it is not clear how N availability from different nitrogen fertilizer types impacts crop yields under different ridge–furrow ratios. In addition, little information is available about the internal efficiency mechanism controlling resource utilization (thermal, water, nitrogen, and radiation). Understanding these mechanisms could provide a scientific basis for optimizing the RFPM system and nitrogen fertilizer type selection.

Therefore, the quantitative effects of different ridge–furrow ratios and nitrogen fertilizer types on the dynamics and distribution of captured heat, water, nitrogen, and radiation resources were investigated in a three-year consecutive experiment. Additionally, we assessed the impact of using the RFPM system with varying ridge–furrow ratios and nitrogen fertilizer types on the growth and yield of winter wheat. Furthermore, we aimed to determine an optimized ratio for ridges and furrows as well as an appropriate type of nitrogen fertilizer that would result in higher winter wheat yields and resource utilization efficiency in the region.

2. Materials and Methods

2.1. Site and Description

Experiments were conducted at Shanxi Agricultural University's Organic Dryland Agriculture Station (37°25′ N, 112°36′ E) in Taigu, Shanxi Province, China. The study covers three consecutive growing seasons from September 2018 to June 2021, during the winter

wheat growing season. Over the past sixty years (1960–2020), the region has experienced an average annual precipitation of 462.9 mm and evaporation of 1002.9 mm, which is typical for a semi-arid agricultural area located on the Loess Plateau. Additionally, the average annual temperature in this area was recorded as 9.9 °C with a sunshine duration of approximately 2550 h and a frost-free period lasting around 176 days per year. The soil texture observed in this study belongs to the cinnamon soils, with a bulk density of 1.29 g cm^{-3}, a field capacity of 23.5%, and a wilting point of 7.3% within the soil profile extending up to 140 cm depth. The effective phosphorus, available potassium, alkaline nitrogen, and organic matter contents within the 30 cm soil profile were 18.44 mg kg^{-1}, 236.87 mg kg^{-1}, 53.76 mg kg^{-1}, and 22.02 g kg^{-1}, respectively. The monthly precipitation, solar radiation, and mean temperature between September 2018 and June 2021 at the experimental site are shown in Figure 1.

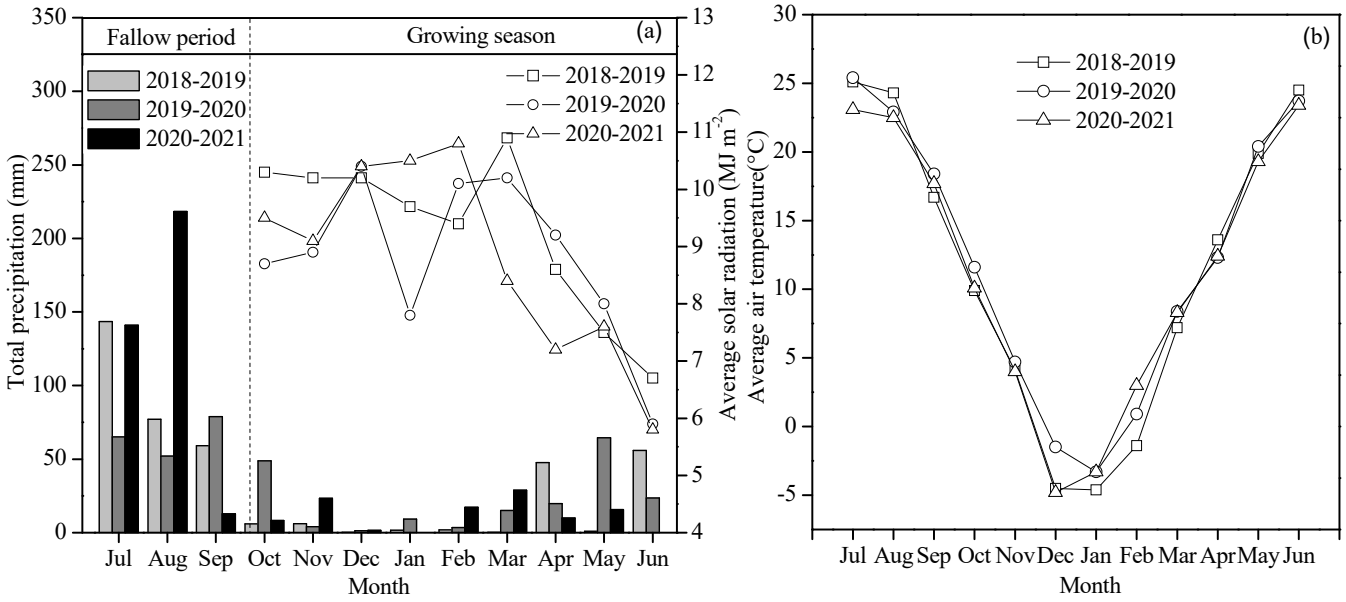

Figure 1. Monthly precipitation and solar radiation (**a**) and monthly mean air temperature (**b**) at the experimental site during the three planting years (2018–2021) of rain-fed winter wheat crops. The monthly precipitation and solar radiation are represented by the bar and line symbols, respectively, in (**a**).

2.2. Experimental Design

The experiment used a split-plot design with three replications. Two types of nitrogen fertilizer, including conventional urea (TU) and controlled-release urea (CRU), were selected for the main plot and four planting patterns (conventional flat planting (F) and the RFPM system with 40 cm furrow widths and 20, 40, and 60 cm ridge widths as subplots). A schematic diagram of the different planting patterns and their unit sizes is shown in Figure 2. A transparent film with a thickness of 0.08 mm was placed over the ridges at the time of sowing and was later removed after the harvest. A minimum distance of 1.0 m was maintained between the plots to ensure minimal interference from water and nutrient migration between adjacent plots.

A basal dressing consisting of pure N, P_2O_5, and K_2O at rates of 180, 150, and 120 kg ha^{-1} was applied before the establishment of the RFPM and F plots, respectively. The nitrogen fertilizers utilized in the experiments included conventional urea (TU) with a minimum N content of 46% and controlled-release urea (CRU) with an N content of 24%, releasing over a period of 90–120 days, from Kingenta Ecological Engineering Co., Ltd., Linshu, China. Each plot covered an area approximately measuring 36 m^2, and the local mainstream variety 'Zhongmai 175' was planted at a density of 150 kg ha^{-1} across all plots. Pests and weeds were strictly controlled during the growing season to avoid yield loss.

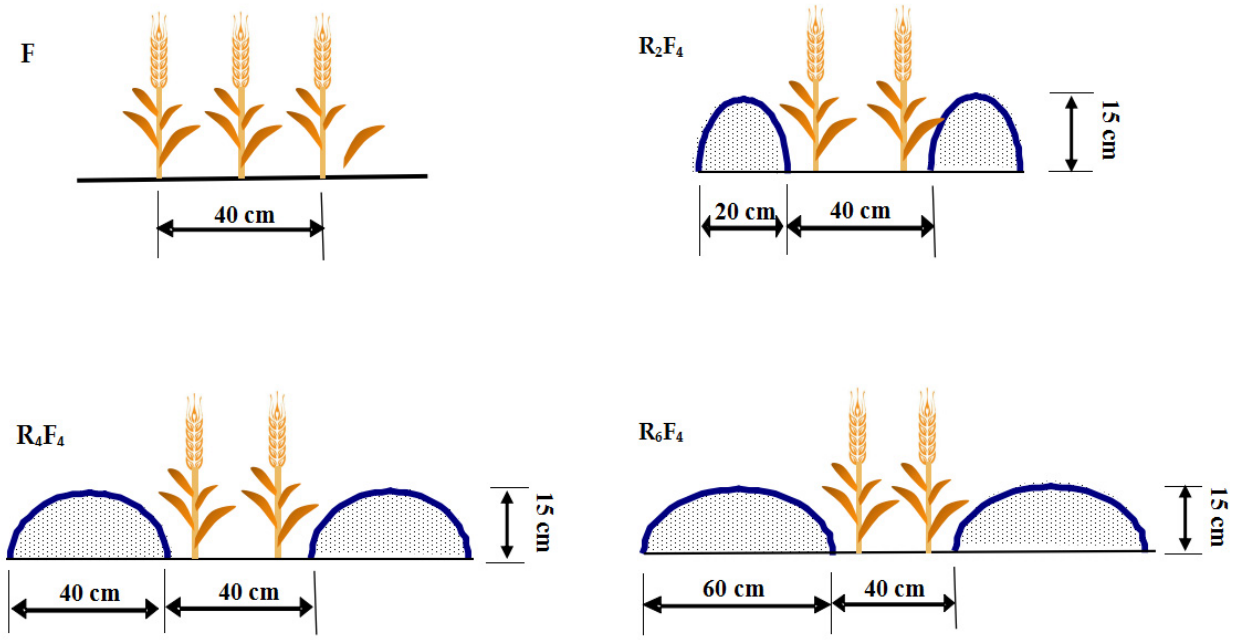

Figure 2. Field schematic diagrams for four planting patterns (F, R_2F_4, R_4F_4, and R_6F_4) and their unit sizes of rain-fed winter wheat.

2.3. Sampling and Measurements

2.3.1. Phenology

The phenology of winter wheat was continuously monitored throughout the entire growing season for each plot. The date was recorded when at least 50% of the plant population in the observation plot had reached various stages, including seedling emergence, re-greening, flowering, and physiological maturity [21].

2.3.2. Soil Temperature and Soil Water Content (SWC)

An automatic soil temperature probe (DS1922L, Analog Devices, Shanghai, China) was buried 15 cm below the surface between two rows of plants in each plot. This instrument provided continuous measurements of soil temperature (°C) at intervals of every 4 h during the entire growth period of wheat.

Soil samples for winter wheat were taken using a hand drill at a depth of 140 cm with sampling points spaced every 20 cm at various stages including sowing, seedling emergence, flowering, grain filling, and maturity. In F treatments, soil samples were taken midway between two rows of wheat. In RFPM treatments, soil samples were collected at three specific locations: the center ridge point, the junction point between the ridge and furrow, and the center furrow point. These soil samples were then placed in an aluminum box and dried in a forced-air oven at a temperature of 105 °C for a duration of 24 h to determine the soil water content (SWC).

2.3.3. Leaf Area Index (LAI) and Accumulation of Dry Matter (DM)

During the main phenological period, a total of twenty plants were selected at random from each plot for the evaluation of the leaf area index (LAI) and the dry matter (DM). The LAI represents the ratio between the overall leaf area of leaves within a plot and the plot's area. The individual leaf area is determined by multiplying a leaf's length with its maximum width, then multiplying the result by 0.75 [22]. To obtain DM, wheat plants were chopped and subjected to drying in a forced-air oven at 105 °C for thirty minutes initially, then maintained at a temperature range of 65–70 °C for at least seventy-two hours.

2.3.4. Grain Yield

At physiological maturity, six rows of 1 m-long wheat plants were harvested manually from the middle of each plot. The grain was then dried in a forced-air oven to determine the moisture content. Finally, the grain yield was calculated at a moisture content of 14% [3].

2.4. Data Calculation

2.4.1. Soil Thermal Time (TT_{soil}) and Thermal Time Use Efficiency (TUE)

The cumulative soil thermal time (TT_{soil}, °C) for winter wheat from sowing to maturity was calculated using the method described by McMaster et al. (1997) [23]:

$$TT_{soil} = \sum(T_{mean} - T_{base}) \quad (1)$$

where T_{mean} represents the daily mean temperature of the soil, while T_{base} denotes winter wheat's basic soil temperature of 0 °C. All the available data with T_{mean} below the basic soil temperature were treated as equal to 0 °C.

The TUE (kg ha^{-1} (°C d)$^{-1}$) for the winter wheat grain yield was calculated according to the method proposed by Subrahmaniyan et al. (2018) [24]:

$$TUE = \text{Grain yield}/TT_{soil} \quad (2)$$

where TT_{soil} (°C d) is winter wheat soil thermal time throughout the growing season.

2.4.2. Intercepted Photosynthetically Active Radiation (PAR_i) and Radiation Use Efficiency (RUE)

The amount of PAR_i (MJ m^{-2}) intercepted by the wheat canopy was computed using Zhang et al.'s (2019) [2] exponential function:

$$PAR_i = \sum 0.5R(1 - e^{-kLAI}) \quad (3)$$

where R (MJ m^{-2}) represents the daily solar radiation, while k denotes the light extinction coefficient (0.65 for winter wheat [25]) and LAI indicates the leaf area index.

The formula proposed by Subrahmaniyan et al. (2018) [24] was used to calculate the RUE (g MJ^{-1}) for the wheat grain yield:

$$RUE = GY/PAR_i \quad (4)$$

where GY (g m^{-2}) is the grain yield of wheat and PAR_i (MJ m^{-2}) is the photosynthetically active radiation intercepted by the leaves during the entire growing season of the winter wheat crop.

2.4.3. Soil Water Storage (SWS), Evapotranspiration (ET), and Water Productivity (WP)

Using the formula introduced by Mo et al. (2017) [12], the indicators of SWS (mm), ET (mm), and WP (kg mm^{-1} ha^{-1}) were calculated as follows:

$$SWS = SD \times SWC \times \rho \quad (5)$$

$$ET = P + \Delta SWS \quad (6)$$

$$WP = GY/ET \quad (7)$$

where SD is the depth of the soil layer (mm), SWC is the water content of a given soil layer (%), ρ is the soil's bulk density (g cm^{-3}), and P corresponds to total precipitation received during the winter wheat growth period (mm), whereas ΔSWS (soil water depletion) indicates variation in stored soil water from sowing to the maturity stage for winter wheat crops (mm).

2.4.4. Partial Factor Productivity of N (PFP_N)

The formula provided by Qiang et al. (2022b) [15] was used to calculate the PFP_N (kg kg^{-1}):

$$PFP_N = GY/IR \quad (8)$$

where GY is the grain yield of wheat (kg ha^{-1}) and IR is the nitrogen input rate (kg ha^{-1}).

2.5. Statistical Analysis

The ANOVA technique implemented through SPSS Statistics 18 (IBM, Chicago, IL, USA) statistical software facilitated assessment of the ridge–furrow ratio's impact along with the nitrogen fertilizer type and planting year on grain yield, resource allocation, and utilization patterns. Significant differences among treatments were compared utilizing the $LSD_{0.05}$ test. Graphics were generated employing Origin 8.5 (OriginLab, Northampton, MA, USA) drawing software.

3. Results

3.1. Dry Matter (DM) Accumulation Dynamics

The planting pattern, nitrogen fertilizer type, and growing season significantly affected the DM (Figure 3). Regardless of the nitrogen fertilizer type and growing season, DM followed the order of $R_6F_4 = R_4F_4 > R_2F_4 > F$ over the whole growth period. The effect of the N fertilizer type on vegetative dry matter accumulation was not significant. However, CRU increased DM levels during the reproductive growth period compared to TU. The DM at maturity value was greatest in the 2020–2021 season, followed by the 2019–2020 and 2018–2019 seasons, with values of 9125.9, 5578.7, and 5175.4 kg ha^{-1}, respectively.

3.2. Leaf Area Index (LAI) Dynamics

The planting pattern, nitrogen fertilizer type, and growing season significantly affected the LAI (Figure 4). Averaged across the nitrogen fertilizer type and growing season, LAI followed the order: $R_6F_4 = R_4F_4 > R_2F_4 > F$ over the whole growth period. Applying CRU significantly increased LAI, particularly during the reproductive growth period. The mean value for LAI was highest during the 2020–2021 season, followed by 2018–2019 and 2019–2020, with values of 2.8, 1.3, and 1.2 m^2 m^{-2}, respectively.

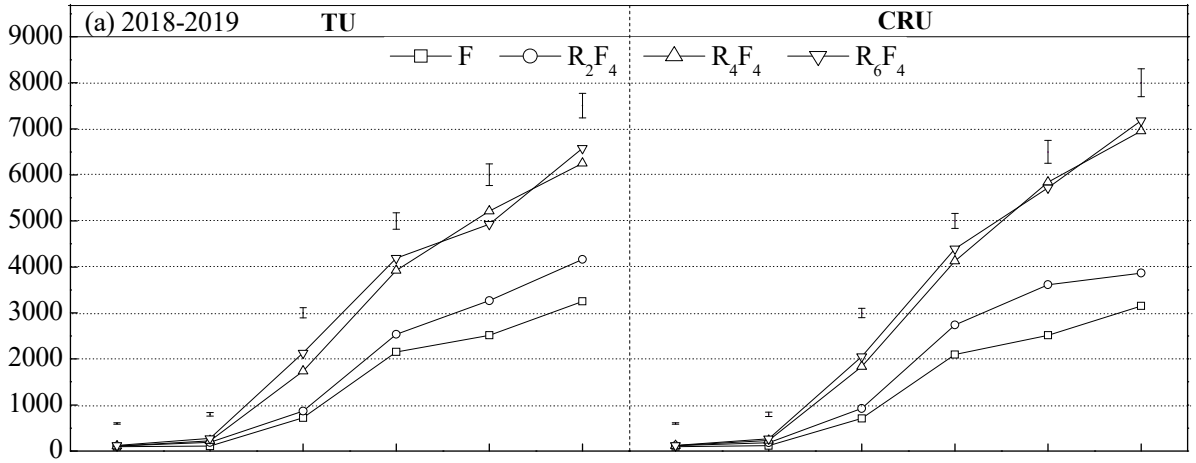

Figure 3. *Cont.*

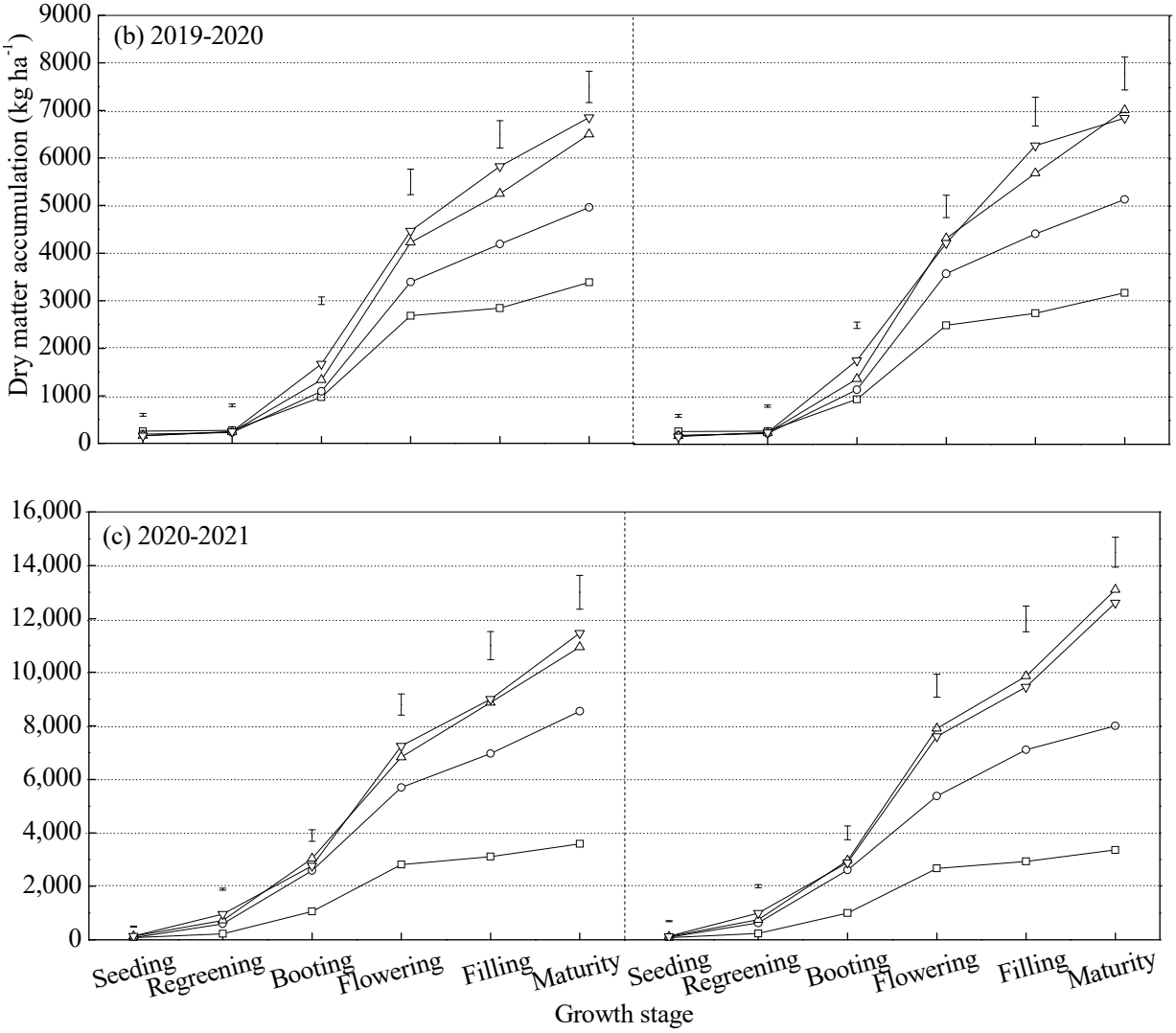

Figure 3. Dynamic of dry matter accumulation for the two nitrogen fertilizer types (TU and CRU) under four planting patterns (F, R_2F_4, R_4F_4, and R_6F_4) over three wheat growing seasons in 2018–2019 (**a**), 2019–2020 (**b**), and 2020–2021 (**c**). Bars are LSDs at $p \leq 0.05$.

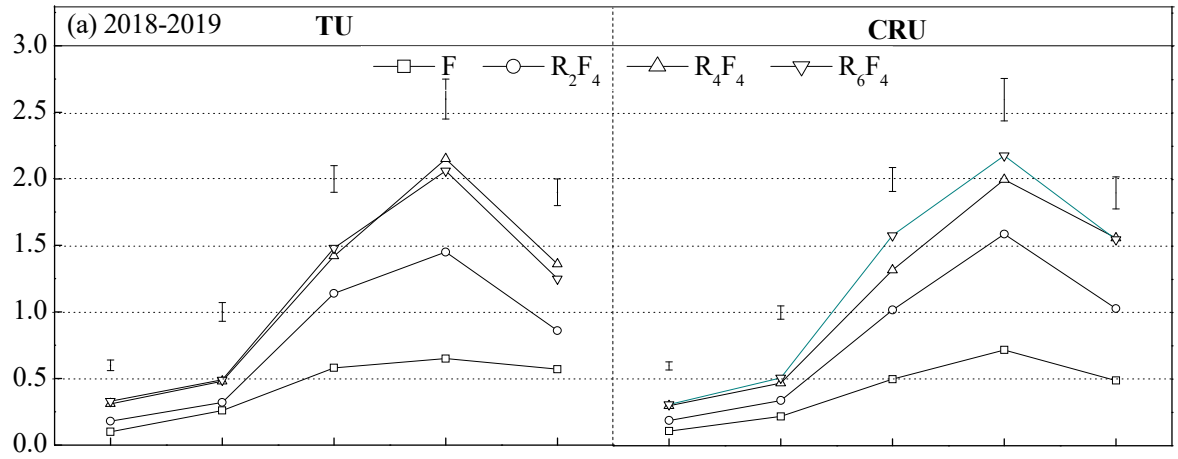

Figure 4. *Cont*.

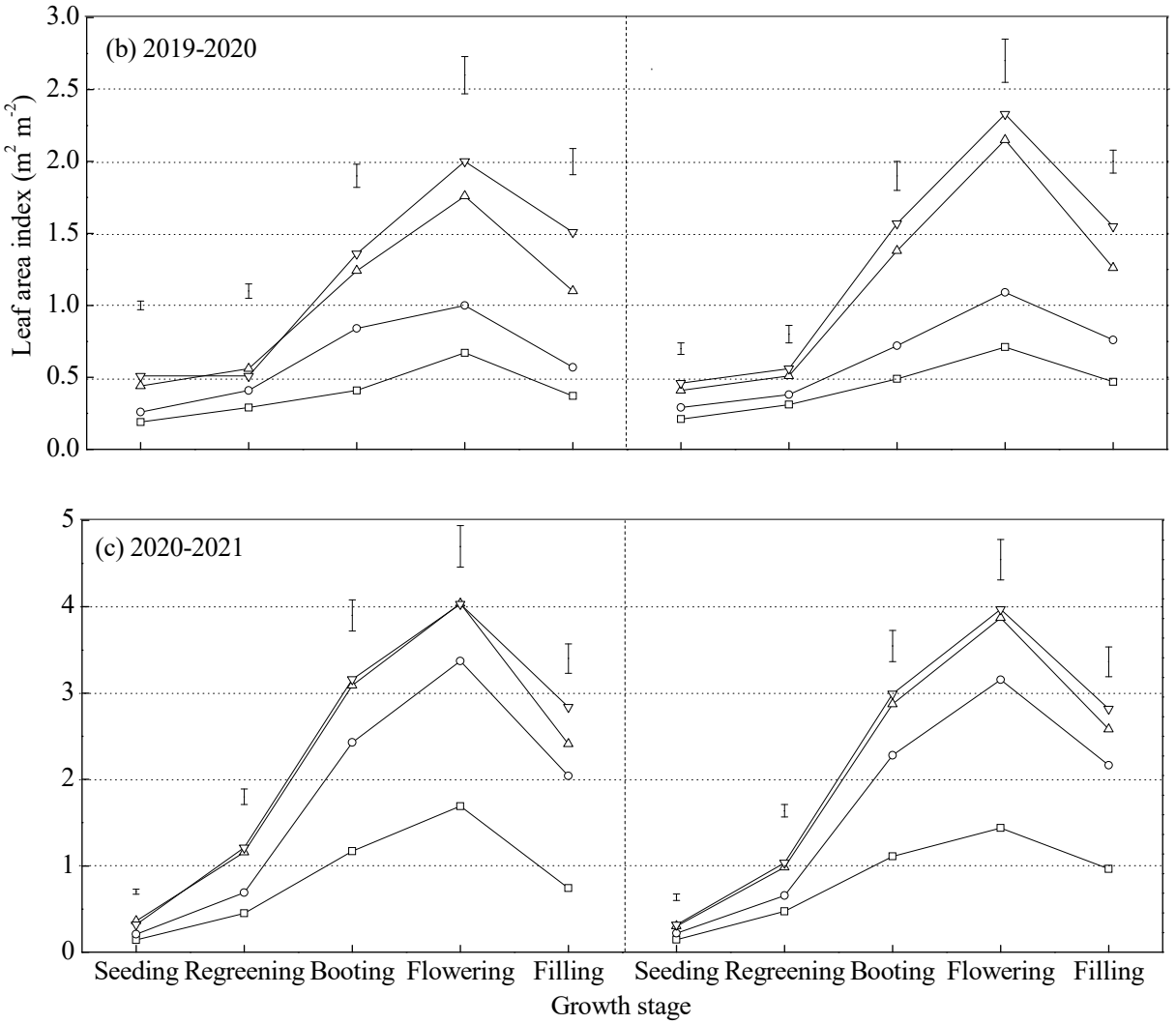

Figure 4. Dynamic of leaf area index for the two nitrogen fertilizer types (TU and CRU) under four planting patterns (F, R_2F_4, R_4F_4, and R_6F_4) over three wheat growing seasons in 2018–2019 (**a**), 2019–2020 (**b**), and 2020–2021 (**c**). Bars are LSDs at $p \leq 0.05$.

3.3. Crop Phenology

The crop phenology was significantly affected by the growing season (Y), nitrogen fertilizer types (NT), and planting patterns (P) (Figure 5). The sowing (So)–seedling emergence (Se) period generally became longer as the ridge–furrow ratio decreased, whereas the opposite occurred for the re-greening (Re)–flowering (Fi) and Fi–maturity (Ma) stages. The CRU extended the total growth period by about 2 days compared to applying TU, and the difference between the two nitrogen fertilizer types was greatest during the Fi–Ma stage. The differences in the meteorological factors meant that the mean value for the length of the whole growing season was longest in 2019–2020, followed by 2018–2019 and 2020–2021, with values of 259, 256, and 252 d, respectively.

3.4. Grain Yield (GY)

Grain yield (GY) was significantly influenced by Y, NT, and P (Figure 6). The average GYs for the 2018–2019, 2019–2020, and 2020–2021 wheat cropping years were 2314.1, 3084.1, and 5699.6 kg ha^{-1}, respectively. The RFPM system produced significantly greater GYs than the F planting treatment. Wheat GY increased with increasing ridge width and was maximized at 40 cm ridge width. Averaged across three growing seasons, CRU increased GY by an average of 11.8% compared to TU.

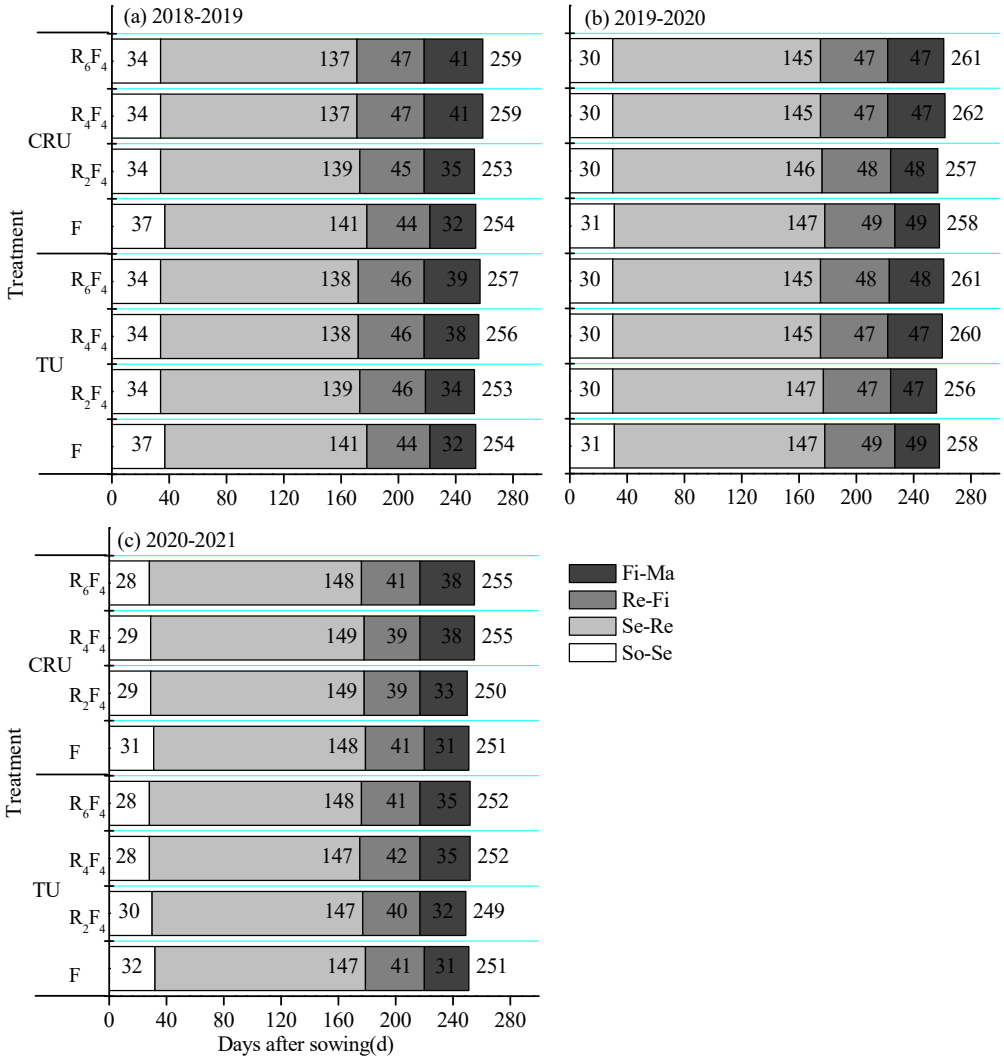

Figure 5. Effect of two nitrogen fertilizer types (NT) and four planting patterns (P) on the number of days from the sowing date to seedling emergence (So–Se), from seedling emergence to the re-greening stage (Se–Re), from the re-greening stage to the flowering stage (Re–Fi), and from the flowering stage to maturity (Fi–Ma) of winter wheat in the 2018–2019 (**a**), 2019–2020 (**b**), and 2020–2021 (**c**) growing seasons.

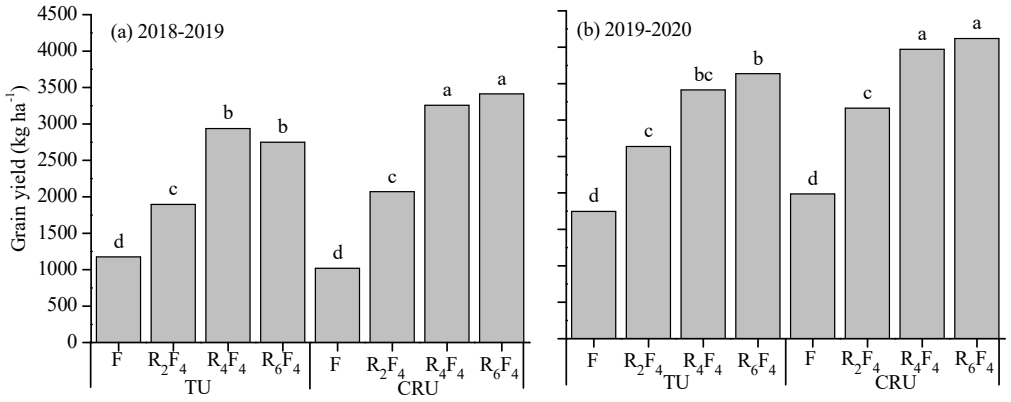

Figure 6. *Cont.*

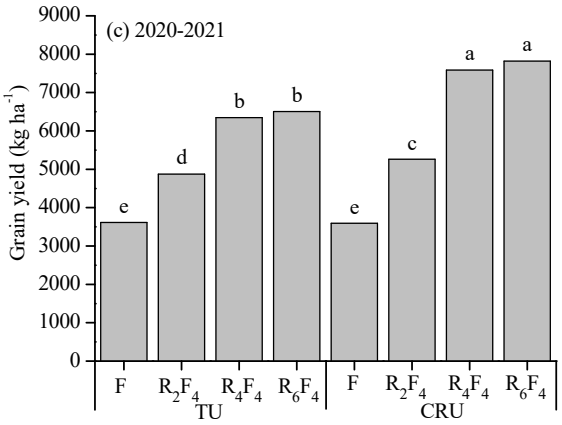

Figure 6. Effect of two nitrogen fertilizer types (NT) and four planting patterns (P) on grain yield over the three winter wheat growing seasons of 2018–2019 (**a**), 2019–2020 (**b**), and 2020–2021 (**c**). Different lowercase letters on the histogram of the same year represent significant differences at the 0.05 probability level for different treatments.

3.5. Resource Use Efficiency

3.5.1. Thermal Time and Radiation Use Efficiency

The thermal time use efficiency (TUE) and radiation use efficiency (RUE) were both significantly affected by Y, NT, and P (Table 1). Both TUE and RUE increased with the ridge–furrow ratio, with mean values of 0.99, 1.47, 1.95, and 1.98 kg ha^{-1} (°C d)$^{-1}$ for TUE, and 0.85, 0.99, 1.14, and 1.14 g MJ^{-1} for RUE in the F, R_2F_4, R_4F_4, and R_6F_4 treatments, respectively. The CRU increased the TUE and RUE values more than TU, with TUE and RUE values of 1.68 kg ha^{-1} (°C d)$^{-1}$ and 1.07 g MJ^{-1}, respectively, for CRU and 1.51 kg ha^{-1} (°C d)$^{-1}$ and 0.99 g MJ^{-1}, respectively, for TU. Averaged across NT and P, the mean TUE values were 0.90, 1.37, and 2.51 kg ha^{-1} (°C d)$^{-1}$ in 2018–2019, 2019–2020, and 2020–2021, respectively, while the mean RUE values were 0.85, 0.93, and 1.30 g MJ^{-1}, respectively.

Table 1. Thermal time use efficiency (TUE) and radiation use efficiency (RUE) were affected by the two nitrogen fertilizer types (NT) and four planting patterns (P) during 2018–2021 rain-fed wheat growing seasons.

NT	P	TUE [kg ha^{-1} (°C d)$^{-1}$]			RUE (g MJ^{-1})		
		2018–2019	2019–2020	2020–2021	2018–2019	2019–2020	2020–2021
TU	F	0.48 e	0.81 f	1.67 d	0.70 de	0.74 e	1.12 e
	R_2F_4	0.76 d	1.19 e	2.23 c	0.80 cd	0.87 cd	1.20 de
	R_4F_4	1.14 bc	1.51 cd	2.83 b	0.96 ab	0.94 bc	1.33 dc
	R_6F_4	1.07 c	1.59 bc	2.85 b	0.89 bc	0.96 abc	1.35 b
CRU	F	0.42 e	0.92 f	1.66 d	0.61 e	0.81 de	1.11 e
	R_2F_4	0.83 d	1.41 d	2.38 c	0.82 cd	1.00 ab	1.25 cd
	R_4F_4	1.23 ab	1.73 ab	3.24 a	1.02 a	1.05 a	1.54 a
	R_6F_4	1.30 a	1.77 a	3.29 a	1.04 a	1.05 a	1.57 a

A significant difference between treatments at the 0.05 probability level is indicated by different lowercase letters following the same column value.

3.5.2. Water Productivity and Partial Factor Productivity of N

The water productivity (WP) and the partial factor productivity of N (PFP_N) were significantly affected by Y, NT, and P (Table 2). Both WP and PFPN rose as the ridge–furrow ratio increased, with mean values of 10.9, 14.9, 19.1, and 19.1 kg ha^{-1} mm^{-1} for WP and 12.2, 18.4, 25.5, and 26.2 kg kg^{-1} for PFP_N in the F, R_2F_4, R_4F_4, and R_6F_4 treatments, respectively.

The CRU increased WP by 7.8% and PFP_N by 14.1% compared to TU. Averaged across NT and P, the mean WP values were 10.7, 13.1, and 24.2 kg ha^{-1} mm^{-1} in 2018–2019, 2019–2020, and 2020–2021, respectively, while the mean PFP_N values were 12.9, 17.1, and 31.7 kg kg^{-1}, respectively.

Table 2. The water productivity (WP, kg ha^{-1} mm^{-1}) and partial factor productivity of N (PFP_N, kg kg^{-1}) were affected by the two nitrogen fertilizer types (NT) and four planting patterns (P) during 2018–2021 rain-fed wheat growing seasons.

NT	P	WP (kg ha^{-1} mm^{-1})			PFP_N (kg kg^{-1})		
		2018–2019	2019–2020	2020–2021	2018–2019	2019–2020	2020–2021
TU	F	6.4 d	8.4 d	18.1 d	6.5 d	9.7 e	20.1 d
	R_2F_4	9.6 c	11.7 c	21.8 c	10.5 c	14.6 d	27.1 c
	R_4F_4	12.7 b	14.8 ab	27.1 b	16.3 b	19.0 bc	35.3 b
	R_6F_4	13.2 ab	15.5 a	26.0 b	15.3 b	20.2 b	36.2 b
CRU	F	5.6 d	9.2 d	16.9 d	5.7 d	11.0 e	19.9 d
	R_2F_4	9.9 c	13.3 bc	22.9 c	11.5 c	17.6 c	29.2 c
	R_4F_4	13.9 ab	16.1 a	29.9 a	18.1 a	22.1 a	42.1 a
	R_6F_4	14.2 a	16.5 a	31.4 a	19.0 a	22.9 a	43.4 a

A significant difference between treatments at the 0.05 probability level is indicated by different lowercase letters following the same column value.

3.6. Distribution of Soil Thermal Time (TT_{soil}), Evapotranspiration (ET), and Intercepted Photosynthetic Active Radiation (PAR) during the Winter Wheat Growing Season

3.6.1. Soil Thermal Time (TT_{soil})

The soil thermal time (TT_{soil}) was significantly affected by Y, NT, and P (Table 3). Averaged across Y and P, CRU significantly increased TT_{soil} over TU, with values of 2363.6 °C d for CRU and 2322.8°C d for TU. The difference was significant during the Fi–Ma stage, but there was no significant difference during the rest of the growth stages. Generally, the RFPM system had higher TT_{soil} values than F, with increases in TT_{soil} of 1.8%, 5.8%, and 6.7% under R_2F_4, R_4F_4, and R_6F_4 compared to F, respectively, when values were averaged across the three seasons. Increasing the ridge–furrow ratio led to a decrease in TT_{soil} during the Re–Fl growth stage, whereas it increased TT_{soil} during the other growing stages. TT_{soil} capture was affected by solar radiati on during the growth period and was highest during 2018–2019 (2541.0 °C d), followed by 2019–2020 (2242.7 °C d) and 2020–2021 (2245.8 °C d). The effects of NT × P and P × Y on TT_{soil} capture throughout the growing season were both significant ($p < 0.05$), which means that the effect of P on this parameter varied significantly with NT and Y. In contrast, NT×Y had no significant effect on TT_{soil} ($p > 0.05$), suggesting that the Y effects on this parameter were similar and independent of TU or CRU.

3.6.2. Evapotranspiration (ET)

The evapotranspiration (ET) during all the growth periods was significantly affected by Y, NT, and P (Table 4). Applying CRU significantly increased ET over TU, with values of 229.8 and 218.8 mm for CRU and TU, respectively. The difference was greatest during the Fi–Ma period. Averaged across Y and NT, ET increased with increasing ridge width, except during So–Se. ET by winter wheat was affected by rainfall and significantly varied among growing seasons. The ET values showed the following trend in the three planting seasons: 2018–2019 < 2019–2020 = 2020–2021, and NT × P effects on ET were not significant ($p > 0.05$), suggesting that the four planting patterns performed similarly in CRU and TU.

Table 3. Soil thermal time (TT_{soil}, °C d) captured during the main growth stages as affected by the two nitrogen fertilizer types (NT) and four planting patterns (P) over the 2018–2019, 2019–2020, and 2020–2021 growing seasons (Y).

Treatment	TT_{soil} Capture at Various Growth Stages				TT_{soil} Capture during Growth Period
	So–Se	Se–Re	Re–Fi	Fi–Ma	
NT					
TU	442.7 a	538.1 a	596.3 a	745.6 b	2322.8 b
CRU	444.2 a	536.8 a	597.6 a	784.9 a	2363.6 a
P					
F	431.7 c	498.4 d	632.0 a	700.3 c	2262.4 c
R_2F_4	440.9 b	529.1 c	595.2 b	738.1 b	2303.4 b
R_4F_4	447.5 a	550.5 b	584.3 b	810.2 a	2392.5 a
R_6F_4	453.8 a	572.0 a	576.4 c	812.3 a	2414.5 a
Y					
2018–2019	470.1 a	513.3 b	672.6 a	885.0 a	2541.0 a
2019–2020	427.7 b	519.9 b	581.2 b	713.9 b	2242.7 b
2020–2021	432.6 b	579.3 a	537.1 c	696.8 c	2245.8 b
ANOVA					
NT	ns	ns	ns	**	**
P	**	**	**	**	**
Y	**	**	**	**	**
NT × P	ns	ns	ns	**	**
NT × Y	ns	ns	ns	**	ns
P × Y	ns	ns	**	**	**
NT × P × Y	ns	ns	ns	**	*

So–Se, from sowing date to seedling emergence; Se–Re, from seedling emergence to re-greening stage; Re–Fi, from re-greening stage to flowering stage; Fi–Ma, from flowering stage to maturity; and So–Ma, from sowing date to maturity. Within the NT, P, and Y treatments, the symbols '*' and '**' mean significant at the level of $p = 0.05$ and 0.01, respectively, and 'ns' means not significant at the level of $p = 0.05$. A significant difference between treatments at the 0.05 probability level is indicated by different lowercase letters following the same column value.

3.6.3. Photosynthetically Active Radiation (PAR)

The photosynthetically active radiation (PAR) interception during the growth period was significantly affected by Y, NT, and P (Table 5). The effect of NT on PAR was greatest during the reproductive growth stages. However, P affected PAR interception throughout the winter wheat growing season. Photosynthetically active radiation interception increased with the ridge–furrow ratio, and the mean values averaged among NT and Y were 243.1, 322.7, 390.1, and 398.1 MJ m^{-2} for F, R_2F_4, R_4F_4, and R_6F_4, respectively. The highest PAR interception occurred in 2020–2021 (427.9 MJ m^{-2}), followed by 2019–2020 (326.5 MJ m^{-2}) and 2018–2019 (261.1 MJ m^{-2}). There was no significant difference ($p > 0.05$) between NT and P in terms of PAR interception, indicating that the positive impact of P on the PAR was the same regardless of the nitrogen fertilizer type.

3.7. Soil Water Depletion

The depletion of soil water during the growing season was significantly influenced by the Y, NT, and P (Figure 7). Averaged over the NT and Y, the depletion of soil water over the three growing seasons was in the following order: 2020–2021 > 2018–2019 > 2019–2020, with values of 130.9, 94.0, and 64.1 mm, respectively. The NT treatment affected soil water depletion within the 40–100 and 100–140 cm soil layers and followed the trend of CRU > TU, but it did not affect soil water depletion in the 0–40 cm soil layer. Soil water

depletion increased with the ridge–furrow ratio, and the mean values averaged among NT and Y were 71.6, 92.9, 108.7, and 112.2 mm for F, R_2F_4, R_4F_4, and R_6F_4, respectively. The results also showed that the difference in soil water depletion was greatest in the 40–140 soil layer.

Table 4. Evapotranspiration (ET, mm) during the main growth stages as affected by the two nitrogen fertilizer types (NT) and four planting patterns (P) over the 2018–2019, 2019–2020, and 2020–2021 growing seasons (Y).

Treatment	ET at Various Growth Stages				ET during Growth Period
	So–Se	Se–Re	Re–Fi	Fi–Ma	
NT					
TU	28.9 a	44.3 a	83.7 a	61.9 b	218.8 b
CRU	28.7 a	45.6 a	87.8 a	67.8 a	229.8 a
P					
F	34.1 a	29.3 c	76.3 c	60.2 c	199.8 c
R_2F_4	28.8 b	43.9 b	83.9 b	63.6 b	220.2 b
R_4F_4	25.7 c	53.2 a	90.4 a	67.5 a	236.9 a
R_6F_4	26.4 c	53.4 a	92.4 a	68.1 a	240.4 a
Y					
2018–2019	42.1 a	42.1 b	54.7 c	71.7 a	210.6 b
2019–2020	29.2 b	35.2 c	108.3 a	58.1 c	230.8 a
2020–2021	15.0 c	57.6 a	94.3 b	64.7 b	231.6 a
ANOVA					
NT	ns	ns	ns	*	**
P	**	**	**	**	**
Y	**	**	**	**	**
NT × P	ns	ns	ns	ns	ns
NT × Y	ns	*	**	**	ns
P × Y	**	*	**	**	ns
NT × P × Y	*	*	ns	ns	ns

So–Se, from sowing date to seedling emergence; Se–Re, from seedling emergence to re-greening stage; Re–Fi, from re-greening stage to flowering stage; Fi–Ma, from flowering stage to maturity; and So–Ma, from sowing date to maturity. Within the NT, P, and Y treatments, the symbols '*' and '**' mean significant at the level of $p = 0.05$ and 0.01, respectively, and 'ns' means not significant at the level of $p = 0.05$. A significant difference between treatments at the 0.05 probability level is indicated by different lowercase letters following the same column value.

Table 5. Photosynthetically active radiation (PAR, MJ m^{-2}) interception during the main growth stages as affected by the two nitrogen fertilizer types (NT) and four planting patterns (P) over the 2018–2019, 2019–2020, and 2020–2021 growing seasons (Y).

Treatment	PAR Interception at Various Growth Stages				PAR Interception during Growth Period
	So–Se	Se–Re	Re–Fi	Fi–Ma	
NT					
TU	6.7 a	180.0 a	94.0 a	52.1 b	332.7 b
CRU	6.9 a	180.6 a	95.8 a	61.0 a	344.3 a
P					
F	3.7 c	144.4 c	63.2 c	31.8 c	243.1 c
R_2F_4	5.6 b	169.3 b	94.5 b	53.3 b	322.7 b
R_4F_4	8.7 a	201.1 a	110.5 a	69.8 a	390.1 a
R_6F_4	9.1 a	206.4 a	111.4 a	71.3 a	398.1 a

Table 5. *Cont.*

Treatment	PAR Interception at Various Growth Stages				PAR Interception during Growth Period
	So–Se	Se–Re	Re–Fi	Fi–Ma	
Y					
2018–2019	6.6 b	131.0 c	75.4 c	48.1 b	261.1 c
2019–2020	8.1 a	170.6 b	99.2 b	48.6 b	326.5 b
2020–2021	5.6 b	239.3 a	110.1 a	72.9 a	427.9 a
ANOVA					
NT	ns	ns	ns	**	**
P	**	**	**	**	**
Y	**	**	**	**	**
NT × P	ns	ns	ns	*	ns
NT × Y	ns	ns	ns	ns	ns
P × Y	*	**	ns	**	ns
NT × P × Y	ns	ns	ns	ns	ns

So–Se, from sowing date to seedling emergence; Se–Re, from seedling emergence to re-greening stage; Re–Fi, from re-greening stage to flowering stage; Fi–Ma, from flowering stage to maturity; and So–Ma, from sowing date to maturity. Within the NT, P, and Y treatments, the symbols '*' and '**' mean significant at the level of $p = 0.05$ and 0.01, respectively, and 'ns' means not significant at the level of $p = 0.05$. A significant difference between treatments at the 0.05 probability level is indicated by different lowercase letters following the same column value.

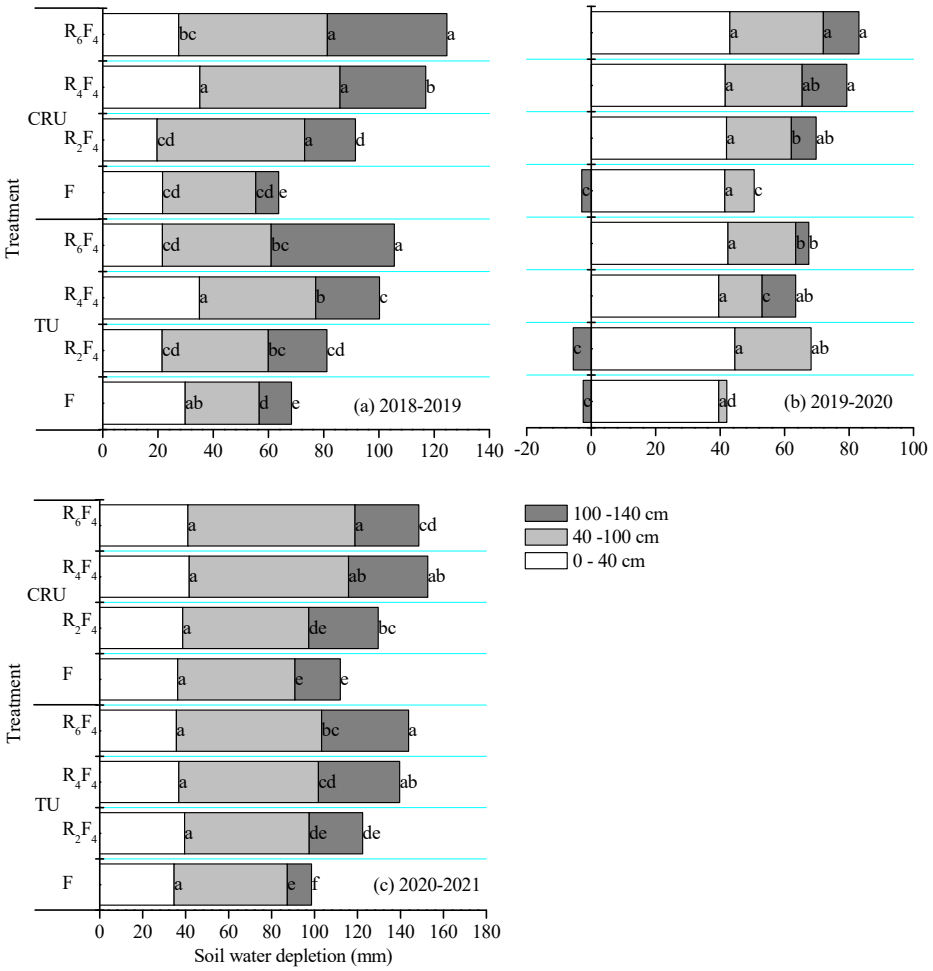

Figure 7. Soil water depletion in the 0–40, 40–100, and 100–140 cm soil layers for the NT treatments (TU and CRU) under the four planting patterns (F, R2F4, R4F4, and R6F4) over the 2018–2019 (**a**), 2019–2020 (**b**), and 2020–2021 (**c**) growing seasons. Different lowercase letters on the same soil layer represent significant differences for the different treatments at the 0.05 level of probability.

4. Discussion

4.1. Crop Growth and Phenology

Soil moisture, nutrients, solar energy, and thermal energy are the key environmental factors affecting crop growth [26,27]. The results from this study showed that the RFPM system significantly increased the LAI and DM compared to F over the three wheat growing seasons. This could be attributed to fact that the RFPM system created favorable hydrothermal conditions in semi-arid areas, which significantly promoted leaf extension and the interception of PAR, thus increasing photosynthetic assimilation and dry matter accumulation [9,11,28]. In addition, the LAI and DM both followed the order: $R_6F_4 = R_4F_4 > R_2F_4 > F$ over the whole growth period. This implied that there was a threshold value for the promotion effect of the RFPM system on crop growth, and excessive ridge widths artificially led to high plant densities in the furrows, which aggravated competition between plants, resulting in premature senescence of the middle and lower leaves of plants and the inhibition of dry matter accumulation [29,30]. The results also showed that CRU increased the LAI and DM, especially during the reproductive growth stage (Figures 3 and 4). This was mainly due to the fact that the CRU application significantly improved soil N availability, especially in the mid and late periods. This delayed leaf senescence and increased DM accumulation [15]. It is well-known that mulching can regulate the relationship between soil moisture and thermal status, thus affecting the crop development process [24,31]. In this study, the RFPM system prolonged the total growth period and the reproductive growth stage by 1–5 days and 1–9 days compared to that of F, respectively (Figure 5). A possible reason for this difference was that the RFPM system significantly improved soil water availability, root activity, the absorption of additional water and nitrogen, and delayed leaf senescence, which prolonged the overall growth period [29,31,32].

4.2. Crop Resource Allocation and Resource Use Efficiency

Numerous studies have shown that crop yield depended on the amount of resources absorbed and the allocation of the resources among different growth stages [27,33]. Consistent with previous studies [2,8], ET in this study increased with the ridge–furrow ratio, except during the So–Se period (Table 4). This was because soil evaporation rather than transpiration determined ET at the seedling stage, and larger ridge widths significantly reduced ET by reducing soil evaporation [6,13]. The TT_{soil} capture values increased with ridge width over the whole growth period, except during the Re–Fi period (Table 3). This was related to the fast crop growth rate and the larger leaf area preventing light from penetrating the leaves and reaching the ground, thus reducing the soil warming effect [2,24]. Photosynthetically active radiation interception at the various growth stages followed the trend of $F < R_2F_4 < R_4F_4 = R_6F_4$ (Table 5). This was mainly due to the superior hydrothermal conditions created by the RFPM system, which improved seedling establishment and subsequent crop canopy development in the RFPM system. This meant that the RFPM system had a higher LAI than that of F (Figure 4), which improved the interception of radiation by leaves [14]. Applying CRU increased the absorption of resources (ET, TT_{soil}, and PAR) compared to TU. Differences were greatest during reproductive growth, as there was no significant difference in N availability between the two N fertilizers during vegetative growth, meaning that differences occurred mainly during late growth [6,15,18].

The ability of plants to capture and utilize resources is the key to determining crop growth and yield [33,34]. In our study, the RFPM system (especially with greater ridge widths) produced higher resource (TUE, RUE, WP, and PFP_N) use efficiencies compared to F (Tables 1 and 2). The effect on TUE may be attributed to the warming effect of the RFPM system in the early growth stage leading to improved early seedling establishment, DM accumulation, and ultimately promoting the transport of dry matter from vegetative organs to grains [2]. The effect on RUE may be attributed to the RFPM system always resulting in higher LAIs compared to the conventional flat planting (F) throughout the growing season (Figure 4). This would increase the interception of solar radiation, the

photosynthetic rate, and ultimately GY [7,28,30]. The effects on WP may be attributed to the RFPM system converting some ineffective rainfall into effective rainfall and to increases in the crop transpiration proportion of ET, which would increase the canopy photosynthetic capacity and ultimately GY [5,8,35]. The effect on PFP_N may be attributable to the RFPM system, particularly when the width is greater, because it improves the soil water conditions. Thus, there was a possible synergistic effect between N and water on the yield performance [4,10,20]. In line with previous research [6,15,18], our study showed that applying CRU led to greater resource use efficiencies than TU.

4.3. Crop Yield

Water scarcity is the main limiting factor for winter wheat productivity in the Loess Plateau rain-fed agricultural area [3,5]. In our study, the RFPM system achieved higher GY than F, possibly because the RFPM system can significantly improve soil moisture availability, minimizing the adverse effects of drought on crop growth [4,13]. Improving the availability of soil moisture has a direct effect on soil temperature and N availability, and ultimately promotes canopy growth and resource utilization, which in turn increases crop yields [2,14,29]. Changing the size of the ridge and furrow is a common measure that is used to regulate resource utilization and crop production. In this study, when the ridge width was $\leq$40 cm, crop yields increased with ridge width. However, there was no effect when the ridge was too wide (>40 cm) because the GY of R_4F_4 was equal to R_6F_4 (Figure 6). This is mainly because increasing the ridge width can significantly improve soil hydrothermal conditions, thus promoting the utilization of resources and ultimately crop yields. However, too wide a ridge wastes the solar energy resources of the rainwater harvesting area (ridge) and exacerbates the competition for resources in the furrow, which is not conducive to yield increases [11,13]. It can be predicted that, beyond a certain point, GY will decrease as the ridge–furrow ratio increases.

4.4. Soil Water Depletion

Crop ET can be significantly increased by using CRU and wider ridges in rain-fed cropping areas [6,36]. At 0–40cm, the planting year affected soil water depletion, but NT and P did not. This may be because the consumption of soil moisture by NT and P in the 0–40 cm soil layer was phased and weak, and the considerable ET due to meteorological factors eventually eliminated any differences. In the 40–100 and 100–140 cm soil layers, a higher ridge–furrow ratio or applying CRU tended to intensify soil water depletion. A potential reason for this was that the RFPM system led to increased root growth depth and root activity [32], which improves the root's ability to absorb moisture from deeper layers of the soil to reduce drought stress [2,12]. Soil moisture in the 0–40 cm layer was easily recovered during the summer fallow period, according to the soil water balance [3,37], but it was not clear whether deep soil moisture (40–140 soil layer) was restored during the fallow period, especially in dry years. Deep soil moisture is an important water source that enables the next stubble crops to cope with periodic drought [38]. Thus, the use of an optimal ridge and furrow size and an appropriate fertilization strategy directly affected the sustainability of rain-fed farmland production.

5. Conclusions

Improving soil water and nutrient availability is important for high yields and resource efficiency in winter wheat farming in the rain-fed agricultural region of the Loess Plateau in China. Implementing RFPM, especially with higher ridge–furrow ratios, facilitated canopy growth and increased its ability to capture more sunlight, resulting in increased evapotranspiration and dry matter accumulation. It also prioritized the allocation of crucial production resources such as water, nitrogen, radiation, and heat towards the reproductive growth phase. These modifications constitute an internal mechanism that drives resource efficiency within the RFPM system and leads to a substantial improvement in winter wheat GY by 51.6–115.2%, TUE by 48.3–99.5%, WP by 37.4–76.3%, RUE by 16.3–34.4%, and PFP_N

by 51.6–115.2% compared to F. Furthermore, applying CRU increased the absorption and utilization of resources compared to TU, particularly during the reproductive growth stage. We suggest that the R_4F_4 treatment combined with CRU could be a suitable integrated resource planting pattern for rain-fed winter wheat production. However, the effect of planting patterns and fertilization strategies on the annual soil moisture balance deserves further investigation, as it has a direct impact on the sustainability of soil moisture.

Author Contributions: Conceptualization, S.Q.; methodology, Y.Z.; software, S.Q., W.L. and X.T.; validation, J.F.; formal analysis, Y.Z.; investigation, Y.Z.; data curation, S.Q., W.L. and X.T.; writing—original draft preparation, S.Q.; writing—review and editing, Y.Z. and J.F.; visualization, Y.Z.; supervision, F.Z. and J.F.; project administration, Z.G., M.S., F.Z. and J.F.; funding acquisition, Z.G. and M.S. All authors have read and agreed to the published version of the manuscript.

Funding: We are grateful for the financial supported by Ministerial and Provincial Co-Innovation Centre for Endemic Crops Production with High-quality and Efficiency in Loess Plateau (SBGJXTZX-35), the National Natural Science Foundation of China (51879226), and Shanxi Agricultural University Science and Technology Innovation Promotion Project (CXGC2023047).

Data Availability Statement: The datasets supporting the results presented in this manuscript are included within the article.

Conflicts of Interest: The authors declare no conflict of interest. The funders had no role in the design of the study; in the collection, analyses, or interpretation of data; in the writing of the manuscript, or in the decision to publish the results.

References

1. Ashraf, M.; Harris, P.J.C. Photosynthesis under stressful environments: An overview. *Photosynthetica* **2013**, *51*, 163–190. [CrossRef]
2. Zhang, X.D.; Kamran, M.H.; Xue, X.K.; Zhao, J.; Cai, T.; Jia, Z.K.; Zhang, P.; Han, Q.F. Ridge furrow mulching system drives the efficient utilization of key production resources and the improvement of maize productivity in the Loess Plateau of China. *Soil Tillage Res.* **2019**, *190*, 10–21. [CrossRef]
3. Sun, M.; Ren, A.X.; Gao, Z.Q.; Wang, P.R.; Mo, F.; Xue, L.Z.; Lei, M.M. Long-term evaluation of tillage methods in fallow season for soil water storage, wheat yield and water use efficiency in semiarid southeast of the Loess Plateau. *Field Crops Res.* **2018**, *218*, 24–32. [CrossRef]
4. Sun, M.Y.; Chen, W.; Lapen, D.R.; Lu, P.N.; Liu, J.H. Effects of ridge-furrow with plastic film mulching combining with various urea types on water productivity and yield of potato in a dryland farming system. *Agric. Water Manag.* **2023**, *283*, 108318. [CrossRef]
5. Gan, Y.T.; Siddique, K.H.M.; Turner, N.C.; Li, X.G.; Niu, J.Y.; Yang, C.; Liu, L.P.; Chai, Q. Ridge-furrow mulching systems-an innovative technique for boosting crop productivity in semiarid rain-fed environments. *Adv. Agron.* **2013**, *118*, 429–476. [CrossRef]
6. Qiang, S.C.; Zhang, Y.; Fan, J.L.; Zhang, F.C.; Sun, M.; Gao, Z.Q. Combined effects of ridge-furrow ratio and urea type on grain yield and water productivity of rainfed winter wheat on the Loess Plateau of China. *Agric. Water Manag.* **2022**, *261*, 107340. [CrossRef]
7. Li, C.J.; Wang, C.J.; Wen, X.X.; Qin, X.L.; Liu, Y.; Han, J.; Li, Y.; Liao, Y.C.; Wu, W. Ridge–furrow with plastic film mulching practice improves maize productivity and resource use efficiency under the wheat–maize double–cropping system in dry semi–humid areas. *Field Crops Res.* **2017**, *203*, 201–211. [CrossRef]
8. Liu, X.L.; Wang, Y.D.; Yan, X.Q.; Hou, H.Z.; Liu, P.; Cai, T.; Zhang, P.; Jia, Z.K.; Ren, X.L.; Chen, X.L. Appropriate ridge-furrow ratio can enhance crop production and resource use efficiency by improving soil moisture and thermal condition in a semiarid region. *Agric. Water Manag.* **2020**, *240*, 106289. [CrossRef]
9. Ali, S.; Xu, Y.Y.; Ahmad, I.; Jia, Q.M.; Ma, X.C.; Sohail, A.; Arif, M.; Ren, X.L.; Cai, T.; Zhang, J.H.; et al. The ridge-furrow system combined with supplemental irrigation strategies to improves radiation use efficiency and winter wheat productivity in semiarid regions of China. *Agric. Water Manag.* **2019**, *213*, 76–86. [CrossRef]
10. Liu, T.N.; Chen, J.Z.; Wang, Z.Y.; Wu, X.R.; Wu, X.C.; Ding, R.X.; Han, Q.F.; Cai, T.; Jia, Z.K. Ridge and furrow planting pattern optimizes canopy structure of summer maize and obtains higher grain yield. *Field Crops Res.* **2018**, *219*, 242–249. [CrossRef]
11. Ren, X.; Cai, T.; Chen, X.; Zhang, P.; Jia, Z. Effect of rainfall concentration with different ridge widths on winter wheat production under semiarid climate. *Eur. J. Agron.* **2016**, *77*, 20–27. [CrossRef]
12. Mo, F.; Wang, J.Y.; Zhou, H.; Luo, C.L.; Zhang, X.F.; Li, X.Y.; Li, F.M.; Xiong, L.B.; Kavagi, L.; Nguluu, S.N.; et al. Ridge-furrow plastic-mulching with balanced fertilization in rainfed maize (*Zea mays* L.): An adaptive management in east African Plateau. *Agric. For. Meteorol.* **2017**, *236*, 100–112. [CrossRef]

13. Li, W.W.; Wen, X.X.; Han, J.; Liu, Y.; Wu, W.; Liao, Y.C. Optimum ridge-to-furrow ratio in ridge-furrow mulching systems for improving water conservation in maize (*Zea may* L.) production. *Environ. Sci. Pollut. Res.* **2017**, *24*, 23168–23179. [CrossRef] [PubMed]
14. Yan, S.C.; Wu, Y.; Fan, J.L.; Zhang, F.C.; Guo, J.J.; Zheng, J.; Wu, L.F.; Lu, J.S. Quantifying nutrient stoichiometry and radiation use efficiency of two maize cultivars under various water and fertilizer management practices in northwest China. *Agric. Water Manag.* **2022**, *271*, 107772. [CrossRef]
15. Qiang, S.C.; Zhang, Y.; Zhao, H.; Fan, J.L.; Zhang, F.C.; Sun, M.; Gao, Z.Q. Combined effects of urea type and placement depth on grain yield, water productivity and nitrogen use efficiency of rain-fed spring maize in northern China. *Agric. Water Manag.* **2022**, *262*, 107442. [CrossRef]
16. Elgharably, A.; Benes, S. Alfalfa biomass yield and nitrogen fixation in response to applied mineral nitrogen under saline soil conditions. *J. Soil Sci. Plant Nutr.* **2021**, *21*, 744–755. [CrossRef]
17. Zhang, H.; Jing, W.J.; Zhao, B.H.; Wang, W.L.; Xu, Y.J.; Zhang, W.Y.; Gu, J.F.; Liu, L.J.; Wang, Z.Q.; Yang, J.C. Alternative fertilizer and irrigation practices improve rice yield and resource use efficiency by regulating source-sink relationships. *Field Crops Res.* **2021**, *265*, 108124. [CrossRef]
18. Liu, Q.F.; Chen, Y.; Liu, Y.; Wen, X.X.; Liao, Y.C. Coupling effects of plastic film mulching and urea types on water use efficiency and grain yield of maize in the Loess Plateau, China. *Soil Tillage Res.* **2016**, *157*, 1–10. [CrossRef]
19. Ke, J.; He, R.C.; Hou, P.F.; Ding, C.; Ding, Y.F.; Wang, S.H.; Liu, Z.H.; Tang, S.; Ding, C.Q.; Chen, L.; et al. Combined controlled-released nitrogen fertilizers and deep placement effects of N leaching, rice yield and N recovery in machine-transplanted rice. *Agric. Ecosyst. Environ.* **2018**, *265*, 402–412. [CrossRef]
20. Kamran, M.; Yan, Z.G.; Jia, Q.M.; Chang, S.H.; Ahmad, I.; Ghani, M.U.; Hou, F.J. Irrigation and nitrogen fertilization influence on alfalfa yield, nutritive value, and resource use efficiency in an arid environment. *Field Crops Res.* **2022**, *284*, 108587. [CrossRef]
21. Zadoks, J.C.; Chang, T.T.; Konzak, C.F. A decimal code for the growth stages of cereals. *Weed Res.* **1974**, *14*, 415–421. [CrossRef]
22. Birch, C.J.; Vos, J.; Van Der Putten, P.E.L. Plant development and leaf area production in contrasting cultivars of maize grown in a cool temperate environment in the field. *Eur. J. Agron.* **2003**, *19*, 173–188. [CrossRef]
23. McMaster, G.S.; Wilhem, W.W. Growing degree days: One equation, two interpretations. *Agric. For. Meteorol.* **1997**, *87*, 291–300. [CrossRef]
24. Subrahmaniyan, K.; Veeramani, P.; Harisudan, C. Heat accumulation and soil properties as affected by transparent plastic mulch in Blackgram (*Vigna mungo*) doubled cropped with groundnut (*Arachis hypogaea*) in sequence under rainfed conditions in Tamil Nadu, India. *Field Crops Res.* **2018**, *219*, 43–54. [CrossRef]
25. Kiniry, J.R.; Sanderson, M.A.; Williams, J.R. Simulating Alamo switchgrass with the ALMANAC model. *Agron J.* **1996**, *88*, 602–606. [CrossRef]
26. Stone, P.J.; Wilson, D.R.; Reid, J.B.; Gillespie, R.N.; Stone, P.J.; Wilson, D.R. Water deficit effects on sweet corn, water use, radiation use efficiency, growth, and yield. *Crop Pasture Sci.* **2000**, *52*, 103–113. [CrossRef]
27. Mwale, S.S.; Azam-Ali, S.N.; Massawe, F.J. Growth and development of bambara groundnut (Vigna subterranea) in response to soil moisture. 2. Resource capture and conversion. *Eur. J. Agron.* **2007**, *26*, 354–362. [CrossRef]
28. Hou, F.Y.; Zhang, L.M.; Xie, B.T.; Dong, S.X.; Zhang, H.Y.; Li, A.X.; Wang, Q.M. Effect of plastic mulching on the photosynthetic capacity, endogenous hormones and root yield of summer-sown sweet potato (*Ipomoea batatas* (L). Lam.) in Northern China. *Acta Physiol. Plant.* **2015**, *37*, 1–10. [CrossRef]
29. Liu, Y.; Yang, S.J.; Li, S.Q.; Chen, X.P.; Chen, F. Growth and development of maize (*Zea mays* L.) in response to different field water management practices: Resource capture and use efficiency. *Agric. For. Meteorol.* **2010**, *150*, 606–613. [CrossRef]
30. Mu, H.D.; Jiang, B.; Wollenweber, B.; Dai, T.; Jing, Q.; Cao, W. Long-term low radiation decreases leaf photosynthesis, photochemical efficiency and grain yield in winter wheat. *J. Agron. Crop Sci.* **2010**, *196*, 38–47. [CrossRef]
31. Jia, Q.M.; Yang, L.Y.; An, H.Y.; Dong, S.; Chang, S.H.; Zhang, C.; Liu, Y.J.; Hou, F.J. Nitrogen fertilization and planting models regulate maize productivity, nitrate and root distributions in semi-arid regions. *Soil Tillage Res.* **2020**, *200*, 104636. [CrossRef]
32. Li, Y.Z.; Yang, J.B.; Shi, Z.; Pan, W.H.; Liao, Y.C.; Li, T.; Qin, X.L. Response of root traits to plastic film mulch and its effects on yield. *Soil Tillage Res.* **2021**, *209*, 104930. [CrossRef]
33. Bu, L.D.; Liu, J.L.; Zhu, L.; Luo, S.S.; Chen, X.P.; Li, S.Q.; Lee Hill, R.; Zhao, Y. The effects of mulching on maize growth, yield and water use in a semi-arid region. *Agric. Water Manag.* **2013**, *123*, 71–78. [CrossRef]
34. O'Connell, M.; O'Leary, G.; Whitfield, D.; Connor, D. Interception of photosynthetically active radiation and radiation-use efficiency of wheat, field pea and mustard in a semi-arid environment. *Field Crops Res.* **2004**, *85*, 111–124. [CrossRef]
35. Negin, B.; Moshelion, M. The evolution of the role of ABA in the regulation of water use efficiency: From biochemical mechanisms to stomatal conductance. *Plant Sci.* **2016**, *251*, 82–89. [CrossRef]
36. Jia, Q.M.; Chen, K.Y.; Chen, Y.Y.; Ali, S.; Manzoor Sohail, A.; Fahad, S. Mulch covered ridges affect grain yield of maize through regulating root growth and root bleeding sap under simulated rainfall conditions. *Soil Tillage Res.* **2018**, *175*, 101–111. [CrossRef]

37. Yu, S.B.; Khan, S.; Mo, F.; Ren, A.X.; Lin, W.; Feng, Y.; Dong, S.F.; Ren, J.; Wang, W.X.; Noor, H.; et al. Determining optimal nitrogen input rate on the base of fallow season precipitation to achieve higher crop water productivity and yield. *Agric. Water Manag.* **2021**, *246*, 106689. [CrossRef]
38. Yang, W.J.; Li, Y.L.; Liu, W.J.; Wang, S.W.; Yin, L.N.; Deng, X.P. Sustainable high yields can be achieved in drylands on the Loess Plateau by changing water use patterns through integrated agronomic management. *Agric. For. Meteorol.* **2021**, *296*, 108210. [CrossRef]